International Journal of Automotive Technology, Vol. 21, No. 4, pp. 795–804 (2020)
DOI 10.1007/s12239–020–0077–9

pISSN 1229–9138/ eISSN 1976–3832

OPTIMIZATION OF THREE-WHEEL VEHICLE ROOF STRUCTURES AGAINST ROLLOVER ACCIDENTS

Jesung Yoo[1)] and Hoon Huh[2)*]

[1)]Division of Future Vehicle, KAIST, Daejeon 34141, Korea
[2)]Department of Mechanical Engineering, KAIST, Daejeon 34141, Korea

(Received 15 December 2017; Revised 27 April 2019; Accepted 29 April 2019)

ABSTRACT–The rollover safety of Three-Wheel Vehicles (TWVs) is critical because of its instability in severe steering, side collisions and flip-over compared to Four-Wheel Vehicles (FWVs). In order to evaluate the rollover safety, the roof crash conditions in various types of accidents are investigated to provide a reliable roof structure. In order to prepare for roof crash conditions for TWVs, investigation has been carried out in aids of multibody dynamic simulations and motion simulations. According to the simulation, the rear region of a TWV's roof crashes onto the pavement in case of the rollover. To design an optimal roof structure of TWVs, topology optimization is utilized based on the roof crash conditions. The preliminary design of the roof structure from topology optimization is modified into eight different designs by changing the shape of a roof structure. In this paper, both a static crash test and a dynamic crash test are simulated to obtain the best design of the roof structure of TWVs. The dynamic crash test of a roof structure is essential because of the rate dependency of materials and evaluation of real crashworthiness. From the preliminary designs, an optimal shape of a roof structure is determined considering possible cases of actual rollover. The optimal shape shows that the front members of the cross-bar reinforcement and window screen member need to be straight and the rear member needs to be arch-shaped.

KEY WORDS : Roof structure, Rollover, Three-wheel vehicle, Strain-rate dependency, Topology optimization

1. INTRODUCTION

In order to cope with the current issue of a global energy crisis and high oil prices, Electric Vehicles (EVs) are widely chosen as a solution to energy savings. EVs exhibit high energy savings and low emission through kinematic energy regeneration system and no power consumption to maintain engine idling. EVs are flexible to have various types of structural design because they do not have an engine room. This structural advantage results from unnecessity of mechanical interaction between the motor and the battery. Three-Wheel Vehicles (TWVs) can offer higher energy efficiency and driving convenience simultaneously retaining the freedom of design of EVs. TWVs possess some major advantages compared to Four-Wheel Vehicles (FWVs). The first advantage is the light weight of TWVs with the reduction of the number of tires. The second advantage is the low rolling resistance due to three wheels. Lastly, TWVs offer a short radius of rotation. These advantages satisfy important needs of customers such as high fuel efficiency and convenience of driving.

In contrast to their advantages, TWVs exhibit the critical weakness of rollover occurrence. This weakness is caused by the short distance between the Center of Mass (CM) and the edge of the base plane as shown in Figure 1, which makes TWVs easy to be rolled over. In addition, the rolling direction of TWVs is different from that of FWVs due to their different rolling axes. This difference causes the exotic behavior of rollovers for TWVs to be different from that of FWV requiring careful consideration in structure design.

Although rollovers are not a common type of accidents, the fatality of rollovers is critical to the passenger safety. In fact, statistical data from the National Highway Traffic Safety Administration (NHTSA) indicate that about 30 % of deaths caused by traffic accidents are the result of rollovers (NHTSA, 2011). These deaths are most often due to the inevitable damage applied to the head and neck of occupants during the rollover accident.

There are many types of research works to reduce this

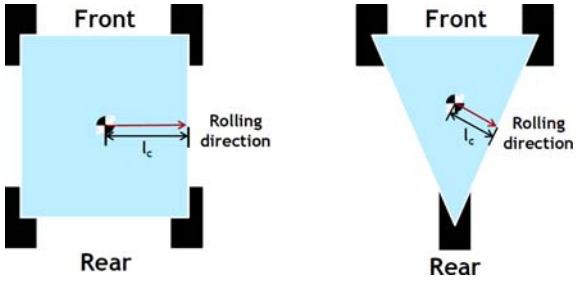

Figure 1. Difference of roll dynamics.

**Corresponding author*. e-mail: hhuh@kaist.ac.kr

significantly high fatality of the rollover accident. According to the report of Mao *et al*. (2007), the effect of the thickness on the roof strength is investigated for a roof panel, a front roof rail and a roof support. The roof strength is increased by only 20 % even if the thickness has doubled. Bernquist (2004) insists that roof structures make the car cage safe when they consist of Ultra High Strength Steel (UHSS) which has the UTS of 1400 MPa. Thanks to UHSS for roof structures, Volvo XC 90 has the highest safety against rollover accidents. However, UHSS has some problems of low formability and high production cost in sheet metal forming. Friedman and Grzebieta (2009) developed HALO^{TM} which is equipment attached to the roof structure for protection against rollover accident. HALO^{TM} achieved successful performance in the rollover tests preventing roof intrusion which can damage the occupants. However, the additional equipment on the roof structure makes the CM higher so that the chance of rollover occurrence could increase. For these reasons, a new type of roof structures has to be designed in order to reduce the fatality of rollover accidents for TWVs.

There are many types of research works to optimize roof structures for high roof strength. Cho and Han (2012) suggested several different alternatives for roof strength enhancement by modification of B pillar, changing materials of roof structures and applying additional reinforcement to roof front header panel. They suggested the shape of reinforcement is the most important for high roof strength considering many alternatives. Han *et al*. (2015) investigated relationship of the roof strength resistance with the displacement of top-end of A-pillar in CRIS test. A commercial code of ADAMS is utilized for simulations of roof crush tests which are quasi-static roof crush test and CRIS rollover test. The effect of roof structures are figured out by several roof crush test simulations and roof strength is turned out to have a relation with a quasi-static roof crush test and a dynamic roof crash test.

In this paper, a new roof structure design for TWVs is carried out against high fatality and occurrence of rollover accidents. At first, roof crash conditions of TWVs are predicted to specify the loading conditions on the roof structure. This procedure is conducted by multibody dynamic simulations and motion simulations by considering side collision, flip-over and yaw induced rollover. Secondly, topology optimization is conducted for preliminary designs of roof structures for TWVs by using the previous loading conditions. These preliminary designs lead to some specific designs of roof structures. Thirdly, static and dynamic simulation for the designs of roof structures is conducted to find the roof structure which satisfies the regulation of roof strength and makes the smallest roof intrusion when it is crashed onto the pavement. With this new roof structure, TWVs can constitute an excellent type of EV due to their high energy efficiency while they are safe from the rollover accident.

2. SIMULATION OF ROOF CRASH CONDITION

In order to design a new roof structure for TWVs, the roof crash conditions of rollovers are identified and prepared for the numerical simulations. The dynamic characteristics of a vehicle depend on the conditions of tires, suspensions, wheelbase, wheel track, wheel alignment and the CM. The rollover occurrence of TWVs with severe steering is investigated with a commercial code of Carsim 8.02. In addition to the severe steering, this section seeks for roof crash conditions of TWVs by motion simulations with other causes of rollovers such as side collisions and flip-over. These kinds of accidents are then analyzed by using multibody dynamic and motion simulations.

2.1. Multibody Dynamic Simulation

In order to examine rollovers of TWVs, multibody dynamic simulations are carried out using the commercial code of Carsim 8.02. The TWV model is classified into two types: Model I; and Model II according to the location of the CM with a configuration and arrangement of the motor and battery as shown in Figure 2. The driving condition of this simulation is a fishhook test at a vehicle speed of 80 km/h. The fishhook test is a specialized method for checking rollover occurrence in case of severe steering (Garrott *et al*., 1999). In this case, the driving force is given by the front wheel and steering is given by the rear wheel. According the results of the multibody dynamic simulation, both TWV models rolls over. Especially for Model II, over-steering is dominant because of the location of its CM, which is closer to the front than that of Model I.

Figure 3 shows sequential images of rollovers obtained from the multibody dynamic simulation. The simulation shows that over-steering takes place first and then the rollover occurs. In order to prepare for roof crash conditions, these results are utilized for motion simulation.

2.2. Motion Simulation

Motion simulation is a technique to predict the dynamic behavior of a rigid body. In order to prepare for the

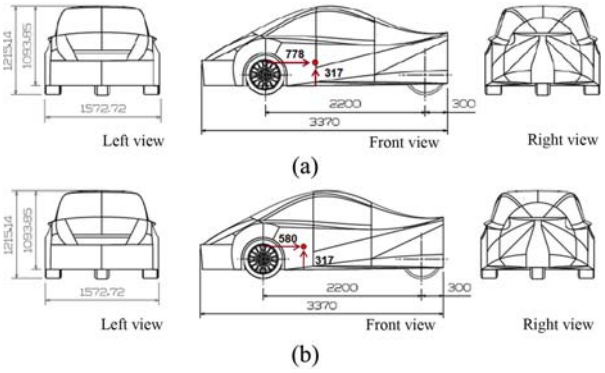

Figure 2. TWV models: (a) Model I; (b) Model II.

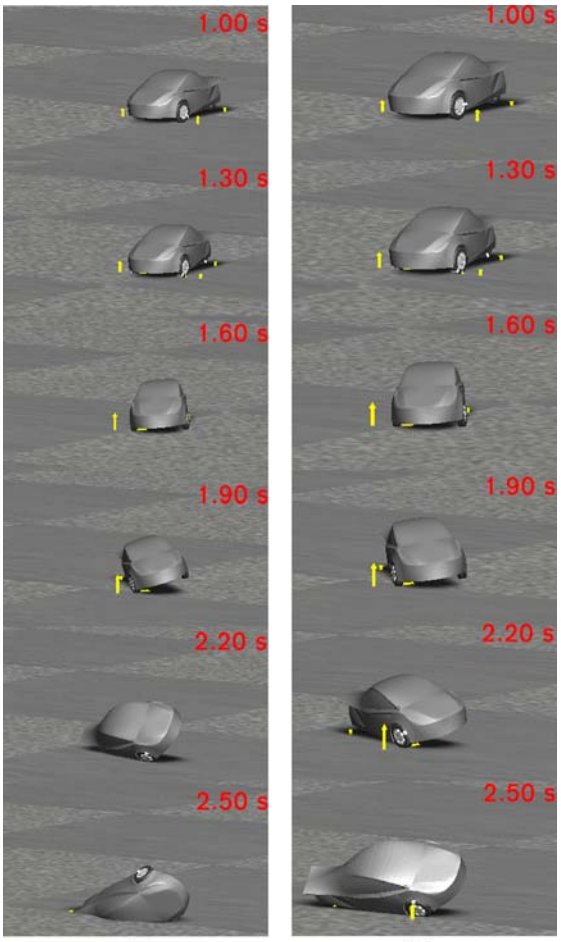

Figure 3. Multibody dynamic simulation results: (a) Model I; (b) Model II.

conditions of a roof crash due to a vehicle rollover, motion simulation constitutes an effective way to elucidate roof crash conditions. Four different types of accidents that lead to rollovers are examined: side collision; weak flip-over; strong flip-over; and yaw induced rollover as shown in Figure 4. For side collision, the initial speed of the side part of the vehicle is set to 18 km/h along the side direction which is the condition of the result from side collision test with a crash speed of 36 km/h. For weak and strong flip-over, the initial speeds of the one side of the wheel are set to 7 km/h and 8 km/h, respectively. The initial speed of 7 km/h makes the left side of the roof structure crashed onto the pavement while that of 8 km/h makes the right side of the roof structure crashed. For yaw induced rollovers, the simulation results from the multibody dynamic simulation are used as severe steering at a vehicle speed of 80 km/h. The commercial code of SolidWorks Motion 2012 is employed for this motion simulation. In order to describe roof crash conditions, a coordinate system is used for the pitch angle and the roll angle as described in Figure 5. The results are presented in Table 1.

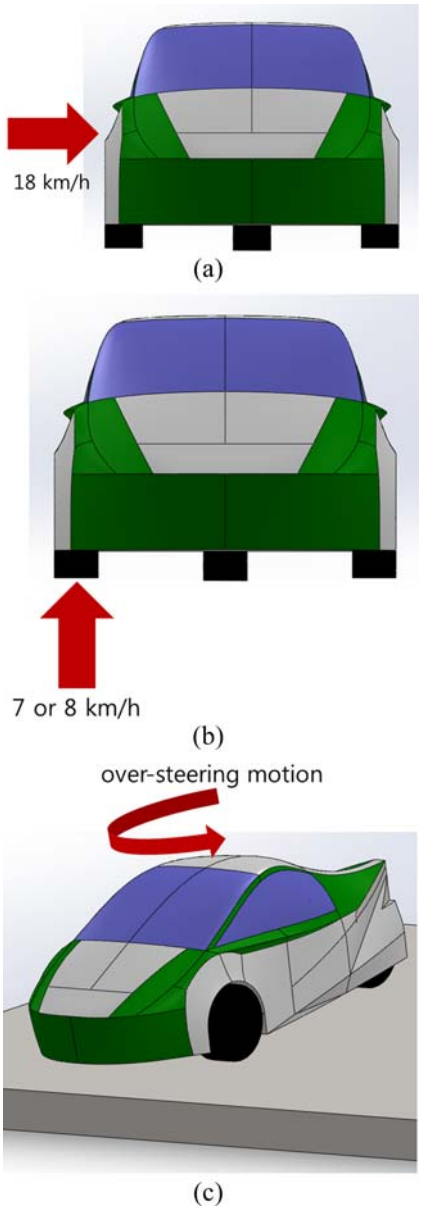

Figure 4. Motion simulation conditions: (a) Side collision; (b) Flip over; (c) Yaw induced.

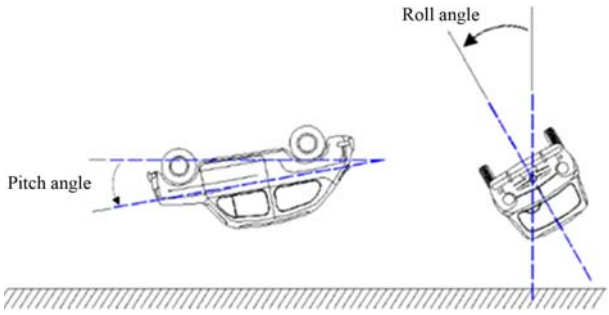

Figure 5. Coordinate system to describe motion simulation results.

Table 1. Motion simulation results.

Conditions	Model I		Model II	
	Pitch angle	Roll angle	Pitch angle	Roll angle
Side collision	− 16.9°	38.8°	− 14.0°	42.3°
Weak flip over	− 14.5°	35.8°	− 14.3°	54.4°
Strong flip over	− 13.3°	26.4°	− 4.1°	38.2°
Yaw induced	− 11.5°	54.1°	6.7°	33.6°

The results show negative pitch angles, except for only one condition. According to the report by Mao *et al.* (2007), FWVs have a positive pitch angle. These differences come from different rolling directions as explained in Figure 1. This different characteristic of the rollover behavior of TWVs points out a critical need to design a new roof structure for TWVs.

3. PRELIMINARY DESIGN OF A ROOF STRUCTURE BY USING TOPOLOGY OPTIMIZATION

3.1. Topology Optimization for Preliminary Design

Topology optimization is a design technique utilized to identify optimal geometric structure under certain conditions by using FE-modeled design space as shown in Figure 6. The overall surface is smooth and has a thickness of 80 mm. The door part and the frame part are separated in optimization, but both are able to make contact with each other. The finite element model has 451,782 tetrahedral elements and 104,185 nodal points. Eight forces are applied to the design space and the amount of force is 22.24 kN which is the maximum force of FMVSS 216 which is the safety regulation specialized for rollover accident (Gatilao *et al*., 2010). The material has an elastic modulus of 210 GPa and a Poisson's ratio of 0.3 with a linear elastic. The objective is to minimize the volume (or the weight) under the design constraint that the maximum stress does not exceed 100 MPa. The objective is to minimize the volume (or the weight) under the design constraint that the maximum stress does not exceed 100 MPa. The constraint value of the maximum stress is calculated to maintain the deformation of the structure which is a quarter of the general elastic limit, 0.2 %, with the safety factor of 4. The optimization procedure is carried out with the commercial code of HyperWorks OptiStruct v11.0.

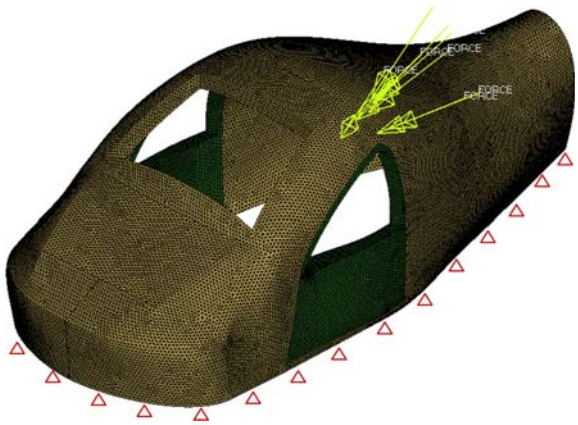

Figure 6. Condition of topology optimizations.

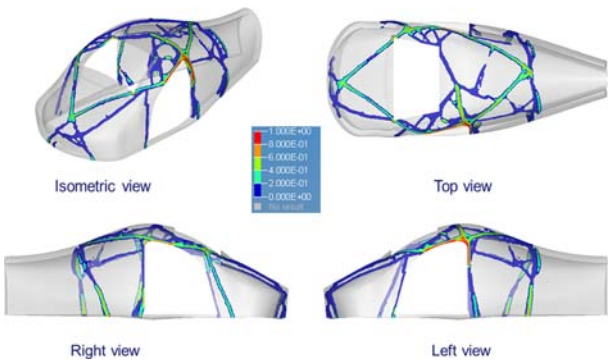

Figure 7. Topology optimization result.

Finite elements with a density less than 0.05 have been removed after the topology optimization as shown in Figure 7. These results are utilized for conceptual and preliminary design. The roof design of a TWV considers

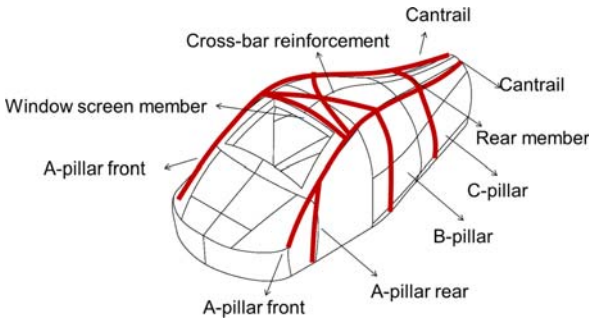

Figure 8. Conceptual design of roof structure for TWV.

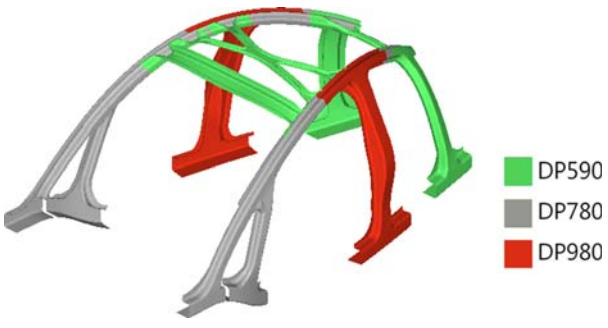

Figure 9. Preliminary design of roof structure for TWV.

A-pillars (front and rear), B-pillars, C-pillars, cantrails, cross-bar reinforcements, a windows screen member and a rear member as shown in Figures 8 and 9. The thickness of the whole members in the roof structure is set to 1.2 mm and the total weight of the roof structures is 36 kg. The material selected is DP980 for the B-pillar to provide additional safety against side collisions. DP780 and DP590 are selected for the different parts considering the existing auto body structure.

3.2. Material Selection and Mechanical Properties

Prior to the simulation of a new roof structure, the dynamic tensile properties of steel have to be identified. According to the report from Huh *et al*. (2010), the material properties with strain-rate dependency have to be taken into account in crash simulation. Dynamic tensile properties are obtained by High Speed Material Testing Machine (HSMTM) as described by H. Huh at KAIST. The materials of DP590, DP780 and DP980 at strain rates ranging from 10^3 s^{-1} to 10^2 s^{-1} have strain-rate dependency as shown in Figure 10.

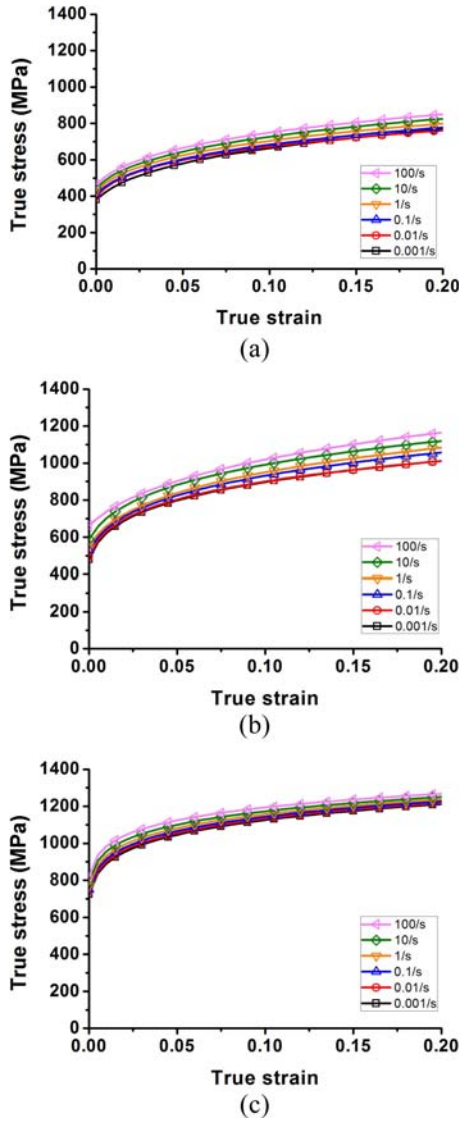

Figure 10. Material properties considering strain rate effect: (a) DP590; (b) DP780; (c) DP980.

4. SIMULATION OF NEW ROOF STRUCTURES

The preliminary design of a new roof structure is modified with three different design variables including a span of the cross-bar reinforcement, a curvature of the front members of a window screen member and cross-bar reinforcement, and a curvature of the rear member. Simulation conditions include static analysis based on FMVSS216 and dynamic analysis based on the inverted vehicle drop test procedure (SAE, 1991), which will be described in the next section.

4.1. Test Methods for the Roof Strength

4.1.1. FMVSS 216

The FMVSS 216 test is a regulation for the roof strength by using a static crushing machine (Gatilao *et al*., 2010). The test is carried out with a maximum force of the machine, 2722 kgf or the appropriate force which is 1.5 times the vehicle's weight. Loading direction is a pitch angle of 5° and a roll angle of 25°. These conditions commonly take place in rollover accidents of FWVs. The test device should crush the vehicle roof no more than 127 mm within 120 s.

4.1.2. Inverted vehicle drop test procedure

The inverted vehicle drop test procedure was suggested by the Society of Automotive Engineers (SAE, 1991). This test method involves suspending the vehicle with some angular conditions and dropping the vehicle. This test constitutes a dynamic condition, and thus strain-rate dependency should be considered.

4.2. Simulation Conditions

4.2.1. Loading conditions

Simulations were conducted with two different cases which include static loading and dynamic loading as shown in Figure 11. The loading direction is a pitch angle of − 10° and a roll angle of 40°, which is a representative condition at an average direction of the motion simulation results. The static case refers to FMVSS 216 with a loading speed of 1 mm/s. For the dynamic condition, the loading speed comes from the motion simulation result which has a maximum crash speed of 3529 mm/s. The FE model has 64,980 QUAD4 shell elements with 35,987 nodes. FE analyses are conducted with a commercial code of LS-DYNA v971.

4.2.2. Model specifications

In order to find the optimal design of a roof structure, a

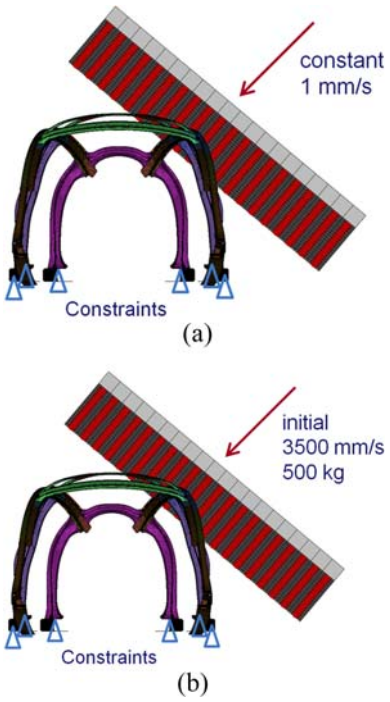

Figure 11. Simulation conditions for a new roof structure: (a) Static test; (b) Dynamic test.

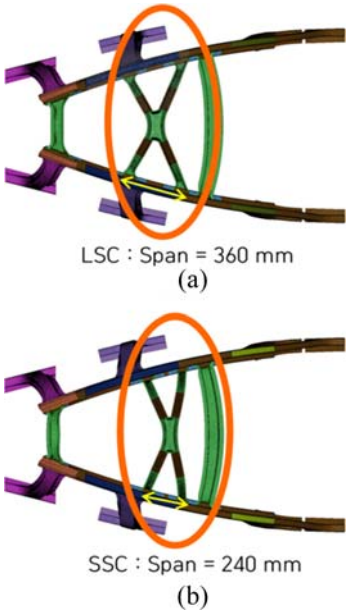

Figure 12. Variations on cross-bar reinforcement: (a) Long span of cross-bar reinforcement; (b) Short span of cross-bar reinforcement.

preliminary design is classified into four different designs with two alternatives as shown in Figures 12 and 13. Figure 12 explains two alternatives with the variation of the span distance: Long Span of Cross-bar reinforcement (LSC); and Short span of Cross-bar reinforcement (SSC)

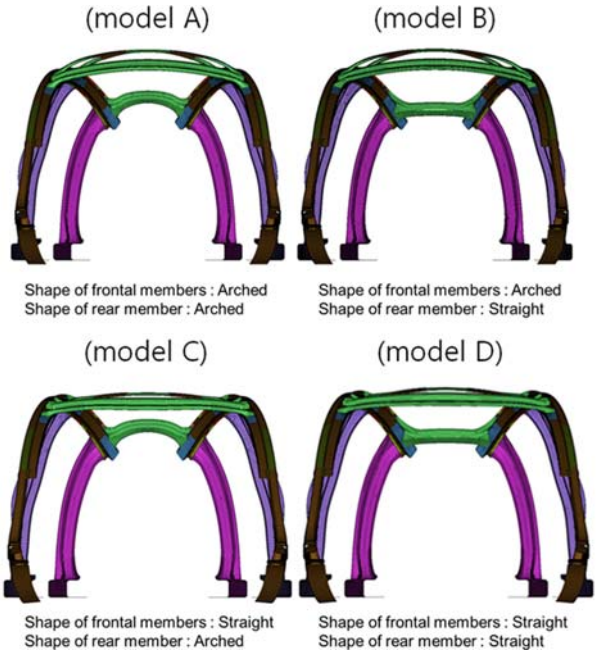

Figure 13. Variations on member structures.

Table 2. Number of elements and nodes for each model.

Type of model	LSC		SSC	
	Number of elements	Number of nodes	Number of elements	Number of nodes
Model A	35,871	36,881	35,398	36,414
Model B	35,614	36,637	35,800	36,818
Model C	35,461	36,422	35,564	36,568
Model D	38,720	39,749	34,980	35,987

according to the span of cross-bar reinforcement. LSC strictly follows the result of topology optimization result while SSC is designed by considering the impact region. Figure 13 explains four different designs. Model A and B have an arched type window screen member and a cross-bar reinforcement; whereas Model C and D have straight type of frontal members. Model A and C have an arched type rear member and Model B and D has a straight type rear member. The number of models for simulation becomes eight and the numbers of elements and nodes for each model is tabulated in Table 2.

4.3. Simulation Results

4.3.1. Evaluation method for simulation

The loading condition of simulation has two different types of static loading and dynamic loading. In the static loading case, simulation followed FMVSS 216 as explained in the Section 4.1. FMVSS 216 states that the roof strength should exceed 1.5 times the weight of the vehicle. For

example, when the weight of a TWV is 500 kg, the roof strength should exceed 7.35 kN. In the dynamic loading case, simulation followed the inverted vehicle drop test procedure. The roof structure is evaluated by the amount of residual roof crush (residual intrusion). The residual roof crush is the maximum displacement of the roof structure after the crash, which is the common safety standard of rollover accidents (Rechnitzer *et al*., 1998; Friedman and Nash, 2001; Hubele, 2009; Yoon *et al*., 2013). In this paper, the maximum interface force and the maximum nodal displacement are used to evaluate the rollover safety of both static and dynamic loading case.

4.3.2. Simulation results of static loading case

Figure 14 shows simulation results after roof structures considered are deformed. All the simulation results show

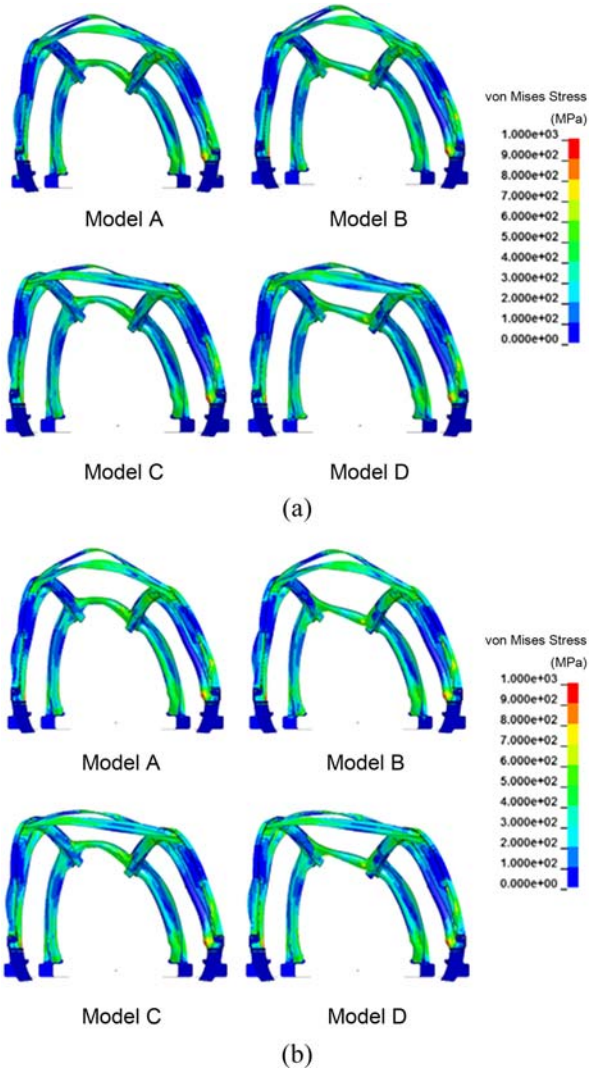

Figure 14. Simulation results of roof structure deformation at the roof intrusion of 120 mm in the static loading case: (a) Long span of cross-bar reinforcement; (b) Short span of cross-bar reinforcement.

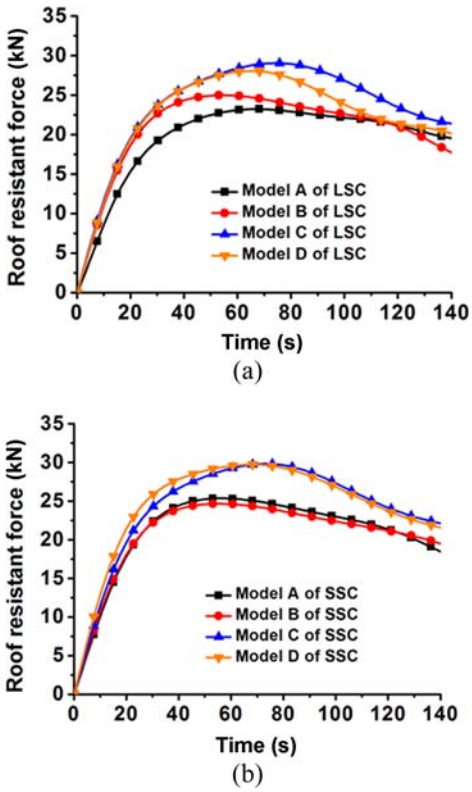

Figure 15. Roof resistant force with respect to time for each model in the static loading case: (a) Long span of cross-bar reinforcement; (b) Short span of cross-bar reinforcement.

the roof structure deformation at the roof intrusion of 120 mm in the static loading case. Figure 15 presents the roof resistant force with respect to time for four Models in each case of Long Span of Cross-bar reinforcement (LSC) and Short Span of Cross-bar reinforcement (SSC). The time axis is equivalent to the displacement axis so that 1 second corresponds to 1 mm. Model C and Model D have higher values of roof resistant force than that of Model A and Model B in both LSC and SSC cases. In the static loading case, simulation results show that the maximum roof resistant forces in all model cases exceed the value of 7.35 kN for the regulation of the roof strength as depicted in Figure 16. The maximum value is 29.82 kN in the case of Model C of SSC and the minimum value is 23.23 kN in the case of Model A of LSC. This means that the roof structure is stable and reliable enough to satisfy the regulation in all cases under the static loading.

4.3.3. Simulation results of dynamic loading case

Figure 17 shows simulation results after roof structures considered are deformed. All the simulation results show the roof structure deformation at the maximum roof intrusion in the dynamic loading case. Figure 18 presents the roof intrusion with respect to time for four Models in

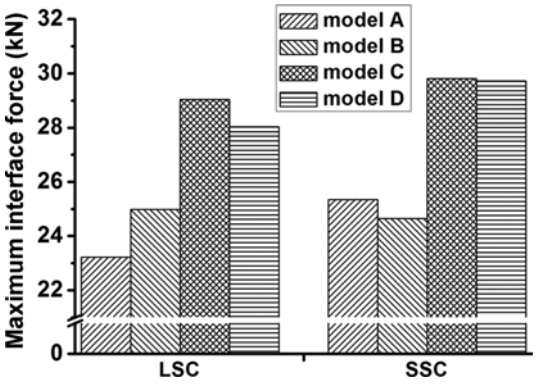

Figure 16. Resultant maximum interface force at each condition in the static loading case.

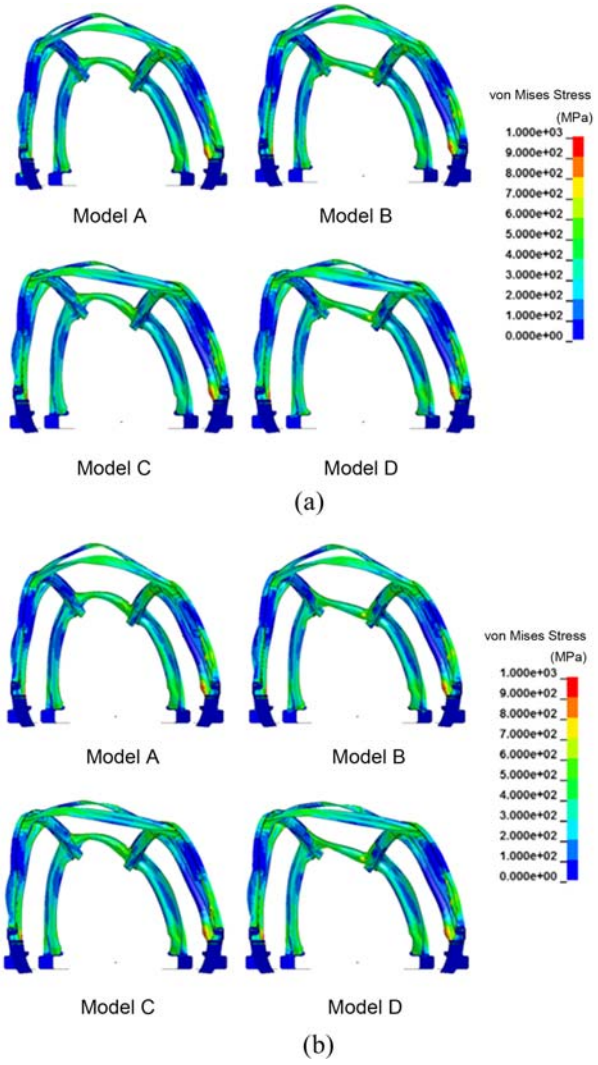

Figure 17. Simulation results of roof structure deformation at the maximum roof intrusion in the dynamic loading case: (a) Long span of cross-bar reinforcement; (b) Short span of cross-bar reinforcement.

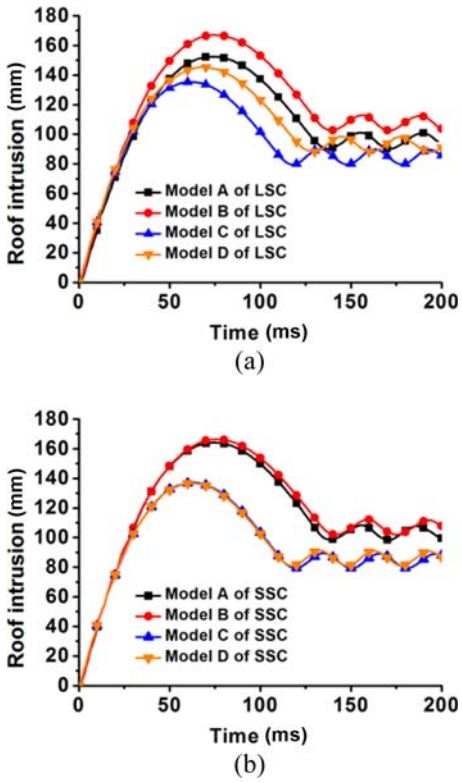

Figure 18. Roof intrusion with respect to time for each model in the dynamic loading case: (a) Long span of cross-bar reinforcement; (b) Short span of cross-bar reinforcement.

each case of Long Span of Cross-bar reinforcement (LSC) and Short Span of Cross-bar reinforcement (SSC). Model C and Model D have a lower value of roof intrusion than that of Model A and Model B. The tendency of this difference is the same as the static loading results in both LSC and SSC cases. In the dynamic loading case, the residual roof intrusion is calculated by the average value of the roof intrusion with respect to time after the impact on the roof structure. Simulation results of the residual roof intrusion are depicted in Figure 19. The minimum value is

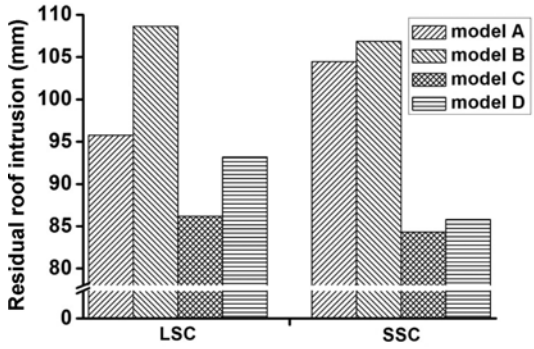

Figure 19. Resultant residual roof intrusion at each condition in the static loading case.

84.33 mm in the case of Model C of SSC and the maximum value is 108.62 mm in the case of Model B of LSC. According to the simulation results, Model C is the most reliable in both LSC and SSC cases.

5. EVALUATION AND DISCUSSION

5.1. Evaluation of the Roof Structure

The residual roof intrusion is the key factor for evaluation of a roof structure (Rechnitzer *et al*., 1998). Although there is no regulation for evaluation of a roof structure considering the residual roof intrusion, Friedman *et al*. (2010) suggested the relation between roof intrusion and fatality of occupants as shown in Figure 20 where the residual roof intrusion is expressed as the residual roof crush. The minimum residual roof intrusion of the new roof structure is calculated as 84.33 mm which is equivalent to 3.3 in. According to Figure 20, the probability of the fatality is 2.64 % in rollover accidents. When the residual roof intrusion is under 3.2 in., the probability of the fatality decreases to 2.03 %.

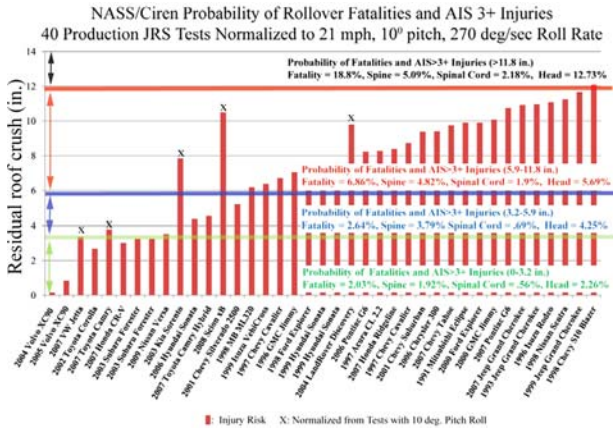

Figure 20. Results of residual roof intrusion for various motor vehicles (Friedman *et al*., 2010).

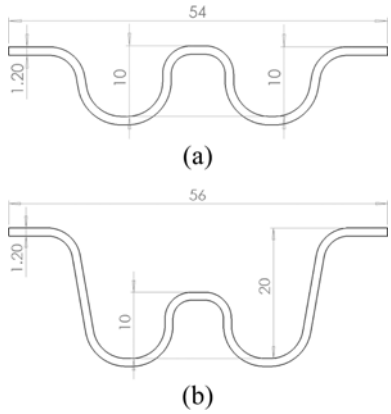

Figure 21. Modification of cross-bar reinforcement in terms of cross-section: (a) Previous design of cross-bar reinforcement; (b) Modified design of cross-bar reinforcement.

In order to satisfy the lowest fatality probability at the residual roof intrusion of 3.2 in. or less, the cross-section of a cross-bar reinforcement can be simply modified as shown in Figure 21. The modification is applied to Model C of SSC which has the lowest value of the residual roof intrusion. Then, the result of the residual roof intrusion decreases to 2.98 in. with the total weight of the structure increased by only 1 kg.

5.2. Effect of the Frontal Member Shape

Model A and B have an arched shape of frontal members which consist of a window screen member and a cross-bar reinforcement while Model C and Model D have a straight shape of frontal members. The simulation results show that Model B has a higher value of the residual roof intrusion than Model D as shown in Figure 22. The amount of buckling of the frontal members is larger in Model B than that in Model D because the buckling initiates earlier with the arched shape of the frontal members than the straight shape. The simulation results imply that the frontal members need to be straight or close to the straight shape in this TWV.

5.3. Effect of Rear Member Shape

Model A and C have an arched shape of a rear member while Model B and D have a straight shape of a rear member. The simulation results show that Model A has a lower value of the residual roof intrusion than Model B as shown in Figure 23. The simulation result of Model A

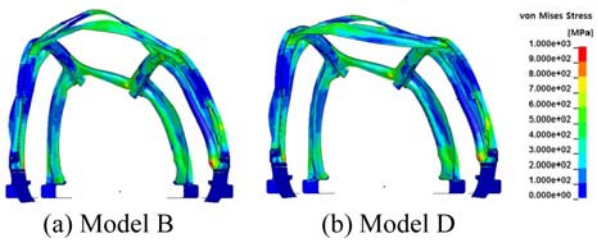

Figure 22. Comparison of frontal members from simulation results with dynamic loading: (a) Model B; (b) Model D.

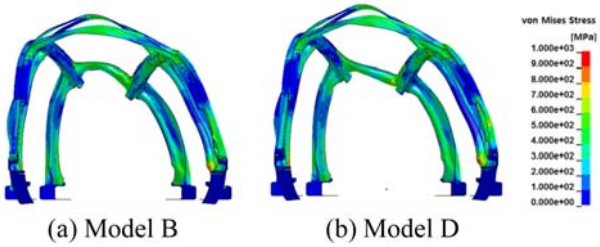

Figure 23. Comparison of rear member from simulation results with dynamic loading: (a) Model A; (b) Model B.

shows that the rear member has deformation of plastic hinge in the dynamic loading case at both end and the middle part while the simulation result of Model B shows that the rear member has deformation of plastic hinge at both ends only. Because of the number of plastic hinges of an arched shape of a rear member, Model A can be considered to absorb higher impact energy in the rear member than Model B. The simulation results imply that the rear member needs to be arch-shaped or close to an arch shape in this TWV.

6. CONCLUSION

TWVs have a high probability of rollover accidents in sever steering, side collision and flip-over. In order to mitigate the fatality in rollover accidents, the roof structure should be optimized for reliable crashworthiness against roof intrusion. The procedure of optimization is specialized for roof structures of TWVs, which consists of multi-body and motion simulations, topology optimization and finite element analysis of a roof structure.

TWVs exhibit several different dynamic characteristics of rollover behavior compared to those of FWVs. The rollover condition on a pitch angle is turned out negative on TWVs from multi-body dynamic and motion simulations, while it is positive on FWVs. The loading conditions calculated by motion simulation are used for topology optimization of TWV roof structures. The design optimization includes a new type of roof structures for a cross-bar reinforcement and a different design of pillar structures. This proposed structure of TWV is divided into four different types of structures according to the shape of member structures and two different type of a cross-bar reinforcement according to the span of a cross-bar reinforcement. The roof structure proposed finally has a low probability of fatality as 2.64 % according to Figure 20. It is noted from the simulation results that the crashworthiness in rollover is enhanced with the frontal member of straight shape and the rear member of an arched shape.

ACKNOWLEDGEMENT–This work was supported by the National Research Foundation of Korea (NRF) grant funded by the Korea government (MSIP) (No. 2010-0028680).

REFERENCES

Bernquist, J. (2004). Safety Cage Design in the VOLVO XC90. American Iron and Steel Institute, Great Design in Steel Seminar, Livonia, Michigan, USA.

Cho, Y. H. and Han, B. K. (2012). Roof strength performance improvement enablers. *Int. J. Automotive Technology* **13**, **5**, 775–781.

Friedman, D. and Grzebieta, R. (2009). Vehicle roof geometry and its effect on rollover roof performance. *Proc. 21st Int. Technical Conf. Enhanced Safety of Vehicles (ESV)*, Paper (No. 07-0361).

Friedman, D. and Nash, C. (2001). Advanced roof design for rollover protection. *Proc. 17th Int. Technical Conf. Enhanced Safety of Vehicles*. Amsterdam, The Netherlands.

Friedman, D., Mattos, G. and Paver, J. (2010). Characterizing the injury potential of a real world rollover. *Proc. ICRASH Conf*., Washington, D.C., USA.

Garrott, W., Forkenbrock, G. and Howe, J. (1999). An Experimental Examination of Selected Manuvers that May Induce On-road Untripped, Light Vehicle Rollover – Phase II of NHTSA's 1997–1998 Vehicle Rollover Research Program. NHTSA. No. HS-808 977, VRTC-86-0421.

Gatilao, F., Roesser, G. and Reaume, B. (2010). An overview of FMVSS 216a – Roof crush resistance testing. *SAE Paper No*. 2010-01-1020.

Han, B. K., Lee, E. D. and Jang, S. M. (2015). Relationship of the roof strength resistance with the displacement of top-end of A-pillar in CRIS test. *Int. J. Automotive Technology* **16**, **4**, 603–610.

Hubele, N. F. (2009). A critical review of some roof crush studies based on rollover field accident data using meta-analysis. *Proc. 19th Canadian Multidisciplinary Road Safety Conf*., Saskatoon, Canada.

Huh, H., Yoon, J. H., Park, C. G., Kang, J. S., Huh, M. Y. and Kang, H. G. (2010). Correlation of microscopic structures to the strain rate hardening of SPCC steel. *Int. J. Mechanical Sciences* **52**, **5**, 745–753.

Mao, M., Chirwa, E. C. and Chen, T. (2007). Reinforcement of vehicle roof structure system against rollover occupant injuries. *Int. J. Crashworthiness* **12**, **1**, 41–55.

NHTSA (2011). Traffic Safety Facts 2009 a Compilation of Motor Vehicle Crash Data from the Fatality Analysis Reporting System and the General Estimates System. National Highway Traffic Safety Administration. 20590.

Rechnitzer, G., Lane, J., McIntosh, A. S. and Scott, G. (1998). Serious neck injury in rollovers – Is roof crush a factor?. *Int. J. Crashworthiness* **3**, **3**, 286–294.

SAE (1991). Inverted Vehicle Drop Test Procedure – SAE J996, Society of Automotive Enginners. J996_199101.

Yoon, H.-S., Lee, K.-T. and Ahn, S.-H. (2013). Measurement of roof deformation caused by vehicle rollover. *Int. J. Automotive Technology* **14**, **4**, 667–674.